Journal of ELECTRONIC MATERIALS, Vol. 44, No. 11, 2015
DOI: 10.1007/s11664-015-4024-x
© 2015 The Minerals, Metals & Materials Society

Evaluation of the Bondability of the Epoxy-Enhanced Sn-58Bi Solder with ENIG and ENEPIG Surface Finishes

WOO-RAM MYUNG,[1] YONGIL KIM,[1,3] and SEUNG-BOO JUNG[2]

1.—SKKU Advanced Institute of Nanotechnology (SAINT), Sungkyunkwan University, 2066 Seobu-ro, Jangan-gu, Suwon 440-746, Republic of Korea. 2.—School of Advanced Materials Science & Engineering, Sungkyunkwan University, 2066 Seobu-ro, Jangan-gu, Suwon 440-746, Republic of Korea. 3.—e-mail: yikim11@skku.edu

The effect of different surface finishes, electroless nickel immersion gold (ENIG) and electroless nickel electroless palladium immersion gold (ENEPIG), on the mechanical properties of Sn-58Bi bumps made with solder paste enhanced with epoxy were investigated. The microstructure and fracture surfaces were observed with scanning electron microscopy, and the compositions of the IMC and solder were measured using energy dispersive spectrometry and an electron probe micro-analyzer (EPMA). To evaluate the mechanical properties, low-speed shear tests and board-level drop tests were performed. The result of the shear tests showed that the bonding strength of the epoxy-enhanced Sn-58Bi solder bumps was higher than that of Sn-58Bi solder for all surface finishes, because of the epoxy surrounding the solder, and the fracture surfaces of epoxy-enhanced Sn-58Bi indicated ductile fracture in the solder joint. However, the result of the drop tests showed that samples with the ENIG and ENEPIG surface finishes had lower drop numbers compared to the sample without these surface finishes. The lower performance resulted from insufficient ejection of epoxy from the ENIG and ENEPIG surface finishes during reflow, which reduced the interfacial bonding area.

Key words: Sn-58Bi solder, epoxy solder, ENIG, ENEPIG, shear test, drop test

INTRODUCTION

The current trend in portable electronic devices means that electronic components need multi-functionality and physical lightness (i.e., lighter, thinner, and smaller, etc.). To meet these trends, industries have been forced to utilize a reliable inter-connection method among delicate electronic components. At the same time, Pb-free materials for joining components are required by the regulation of certain hazardous substances (RoHS);[1] waste electrical and electronic equipment (WEEE)[2] is another challenging issue for electronic industries.[3,4]

The changing specification and restriction in materials for electronic devices have promoted the development of lead-free solders, such as Sn-Ag, Sn-Cu, Sn-Ag-Cu, and Sn-Bi alloys, etc.[5–10] Among them, Sn-Bi alloys have been attractive candidates as solder alloys due to their low melting temperature, low cost, and good mechanical properties such as tensile strength and creep resistance compared to those of the conventional Sn-Pb alloys.[11–13]

The binary Sn-Bi alloy has a eutectic composition at 58 wt.% Bi and this eutectic alloy has a low melting temperature of 138°C, implying a relatively low reflow temperature.[14] This low-temperature reflow, i.e., low soldering temperature, is inevitable for current portable electronic devices because the electronic components and board materials are vulnerable to thermal damage if they are exposed to a high-temperature reflow process. Also, low-temperature reflow is necessary in order to reduce the risk of warpage problems in the flexible printed circuit board (PCB) substrate, which usually induces alignment problems of components during the

(Received January 14, 2015; accepted August 28, 2015; published online September 14, 2015)

surface-mounting process and the mismatch of the coefficients of thermal expansion (CTE) between different materials in electronic packages.[15–18]

However, besides exhibiting a desirable low reflowing temperature, Sn-Bi alloys have a critical property issue of brittleness, which can be a critical problem for solder joints in portable devices.[19]

In order to compensate for this disadvantage of Sn-Bi alloys, it has been shown that adding small amounts of Ag can refine the microstructure of the Sn-58Bi alloys through the formation of "Ag_3Sn" compounds and thereby improve their plasticity.[20] Several reports have also shown that an elongation property can be increased by 20% by adding 0.5–1 wt.% Ag without any noticeable increase in the melting temperature.[21–24]

Another complementary solution for reducing brittleness is the addition of epoxy in Sn-Bi alloys, which can enhance the bonding of the solder with the bonding pad by the formation of an epoxy wall surrounding the solder after the reflow process. In our previous study, shear and drop tests were carried out with the Sn-58Bi solders with/without epoxy enhancement with an organic solderability preservative (OSP) surface finish; these studies showed that the addition of epoxy enhanced the bonding strength of Sn-58Bi solder joints.[25]

In the present study, in order to confirm the sustaining role of epoxy enhancement in Sn-58Bi solder with different surface finishes in the bonding strength, two conventional surface finishes for Pb-free solder joints, i.e., electroless nickel immersion gold (ENIG) and electroless nickel electroless palladium immersion gold (ENEPIG), were employed and compared. In order to evaluate the mechanical properties, a shear test and board level drop test were carried out, followed by the observation of microstructures and interfaces using a scanning electron microscope (SEM), an electron probe microanalyzer (EPMA), and an energy dispersive spectroscope (EDS).

EXPERIMENTAL

Materials and Sample Preparation

To fabricate the solder bump, two types of eutectic Sn-58Bi solder paste [Sn-58Bi solder paste (SB; TLF-401-11; Tamura, Japan) containing 9.4% flux and Sn-58Bi epoxy solder paste (SBE; SAM10-401-27; Tamura) with 14.7% flux including epoxy] were used in the current study. The viscosities of the SB and the SBE were 210 Pa s and 234 Pa s, respectively. PCB substrates were prepared without a surface finish and with two different surface finishes on Cu bonding pads, i.e., ENIG (5 μm Ni-P and 0.08 μm Au) and ENEPIG (5 μm Ni-P, 0.1 μm Pd, and 0.08 μm Au), as shown in Fig. 1. The diameter of the bonding pad was about 200 μm for the shear test and about 380 μm for the drop test samples. The SB and SBE were applied using the stencil printing method and then reflowed. The reflow was conducted using a four-zone IR reflow machine (RF-430-N2; Japan Pulse Laboratory, Japan) for the total reflow time of 5 min with the peak temperature of 190°C. After reflow, solder bumps with the approximate diameter of 225 μm and a height of 190 μm were formed. The height of the epoxy wall surrounding the solder bump was about 75 μm. Sample identification depending on surface finishes and with/without epoxy is summarized in Table I.

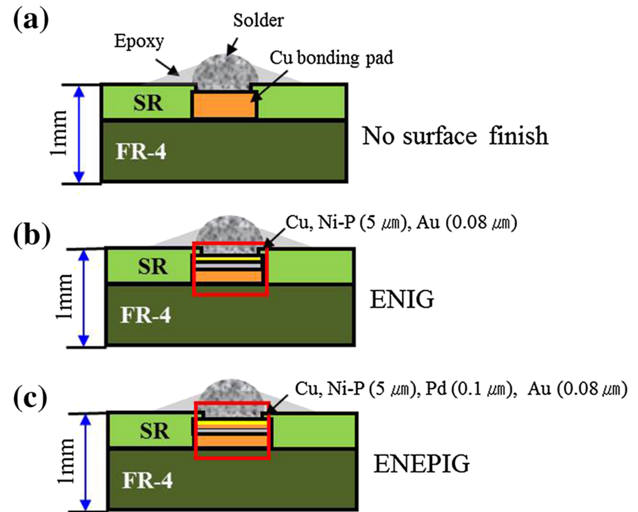

Fig. 1. Samples (a) without surface finish and with (b) ENIG, and (c) ENEPIG surface finishes.

Table I. Sample identification

Solder paste	Surface finish	Sample identification
Sn-58Bi	No	SB
Sn-58Bi with epoxy	No	SBE
Sn-58Bi	ENIG	SB-ENIG
Sn-58Bi with epoxy	ENIG	SBE-ENIG
Sn-58Bi	ENEPIG	SB-ENEPIG
Sn-58Bi with epoxy	ENEPIG	SBE-ENEPIG

Mechanical Tests (Shear and Drop Test)

For the shear test, a substrate was prepared with a solder mask defined (SMD)-type FR4 laminate of 30 × 10 × 1 mm^3 in size, and the nominal size and shape of the solder bonding pads were defined through a 200-μm-diameter circular opening of 1-mm pitch. A low-speed shear test was conducted using a global bond tester (PTR-1000; Rhesca, Japan) with the shear speed of 0.2 mm/s. The tip of the shear tester was placed near the solder ball at 30 μm above the surface of the substrate.

A 15 × 15 × 1 mm^3 SMD type FR4 substrate with 64 (8 × 8 arrays) I/O bonding pads as the component part was prepared for the drop test. The size of the bonding pad opening was 380 μm and the pitch was 1600 μm. The size of the board substrate

was $132 \times 77 \times 1$ mm^3, in compliance with the JEDEC standard 22-B111, having the same bonding pad configuration as that of the component substrate. The drop test was carried out using a drop tester (SD-10; LAB, Japan) and the acceleration peak was 900 G with a pulse duration of 0.7 m/s (JEDEC STANDARD 22-B104-B). The overall process for the drop test and the failure criterion were described in the previous study,[25] and for the comparison of bonding strength depending on the type of surface finish, the total drop numbers without failure were counted and then averaged.

Microstructure Observation

To examine the microstructures of the intermetallic compounds (IMCs) formed at the interfaces of the solder joints and the fracture surfaces after the shear test and board level drop test, samples were investigated and analyzed using SEM (S-3000H; Hitachi, Japan). Chemical compositional analysis and an elementary mapping were carried out using EDS (EMAX-7021-H; Horiba, UK) and/or EPMA (JXA-8500F; JEOL, Japan).

RESULTS AND DISCUSSION

Compared to the sample with no surface finish, the shear strength was not significantly affected by applying ENIG and ENEPIG surface finishes in either the SB and SBE samples. However, the SBE samples showed increased values in both the shear strength and the fracture energy compared to the SB samples, as shown in Fig. 2a and b, respectively. With the addition of epoxy, the shear strength values increased by about 2 times and the fracture energy increased approximately 3–4 times in both the ENIG and ENEPIG samples. As shown Fig. 3, since the shear test was performed at the height of 30 μm from the substrate surface, the tip of the shear tester first collided with the epoxy wall rather than with the solder ball. The fracture occurred in epoxy first and then the fracture was propagated inside the solder during shear test. Since the bonding areas of epoxy with the substrate are much larger than those of the solder with only the bonding pad (about 8–9 times), the epoxy bonding effect may override the surface finish effects in the results of shear strength and fracture energy of solder joints. This role of epoxy in the enhancement of solder bonding strength is clearly shown in Fig. 4, which shows SEM micrographs of the top view of fractured surfaces after the shear test. All samples were fractured through the solder matrix, and in the SBE samples, the solder resists (SR) were skinned off with epoxy regardless of the types of surface finish. This skinned-off effect of the solder resist indicates the strong bonding between the epoxy and the SR, and thereby contributes to the overall increase in

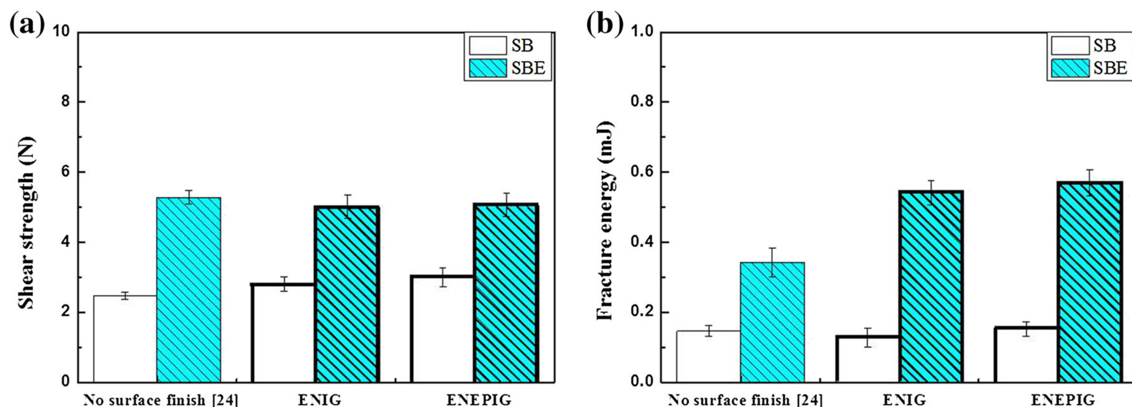

Fig. 2. (a) Shear strength and (b) fracture energy of samples with no,[24] ENIG, and ENEPIG surface finishes.

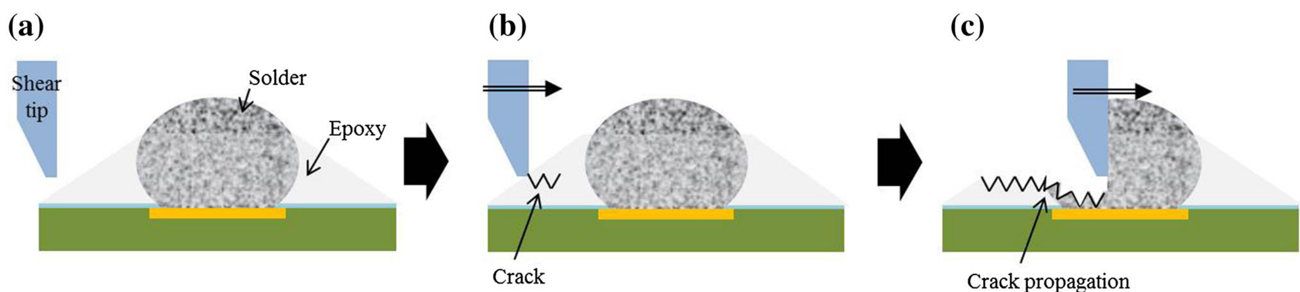

Fig. 3. Schematics of shear test process on Sn-58Bi epoxy solder: (a) shear tip 30 μm above the substrate surface, (b) shear tip collided with the epoxy, (c) shear tip passed through the solder.

both shear strength and fracture energy. Magnified views of the fracture surfaces (red and yellow insets) and the overall shapes of the fracture surfaces show the smear-out of the solder matrix in the direction of the shear test and mostly ductile fracture, which may be partially induced by the low shearing speed.[5,26]

As shown in Fig. 5, however, the results of the drop test of the SBE samples revealed a noticeable variation in the numbers of drops depending on surface finishes. Here, the big deviation in each sample group was caused by the test board configuration; the board substrate was fabricated in compliance with the JEDS 22-B111. The component located at the center received relatively larger flexural stress than component located at the edge which was supported by fixing pins at the four corners. Thus, a big deviation in each sample group occurred. The number of drops of the SBE sample was twice that of the SBE-ENIG and SBE-ENEPIG samples. Since the contributory degree of the epoxy on the bonding strength of solder joints is the same regardless of the type of finish, since epoxy–SR bonding around solders is the same for all samples regardless of the surface finish, it can be deduced that these differences may have originated from the different bonding strengths between the SBE solders and the bonding pads with ENIG and ENEPIG surface finishes. Additionally, because the SR opening (the size of the bonding pad) for the drop test samples (380 μm) is about three times that of the shear test samples (200 μm), the contributory degree to bonding strength by the different surface finishes in the drop test could be more significant than that in the case of the shear test. When compared with the sample with no surface finish from

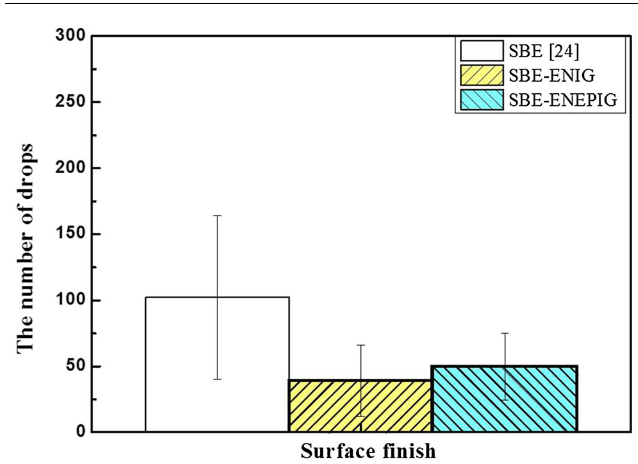

Fig. 5. The number of drops of SBE samples depending on no, ENIG, and ENEPIG surface finishes.

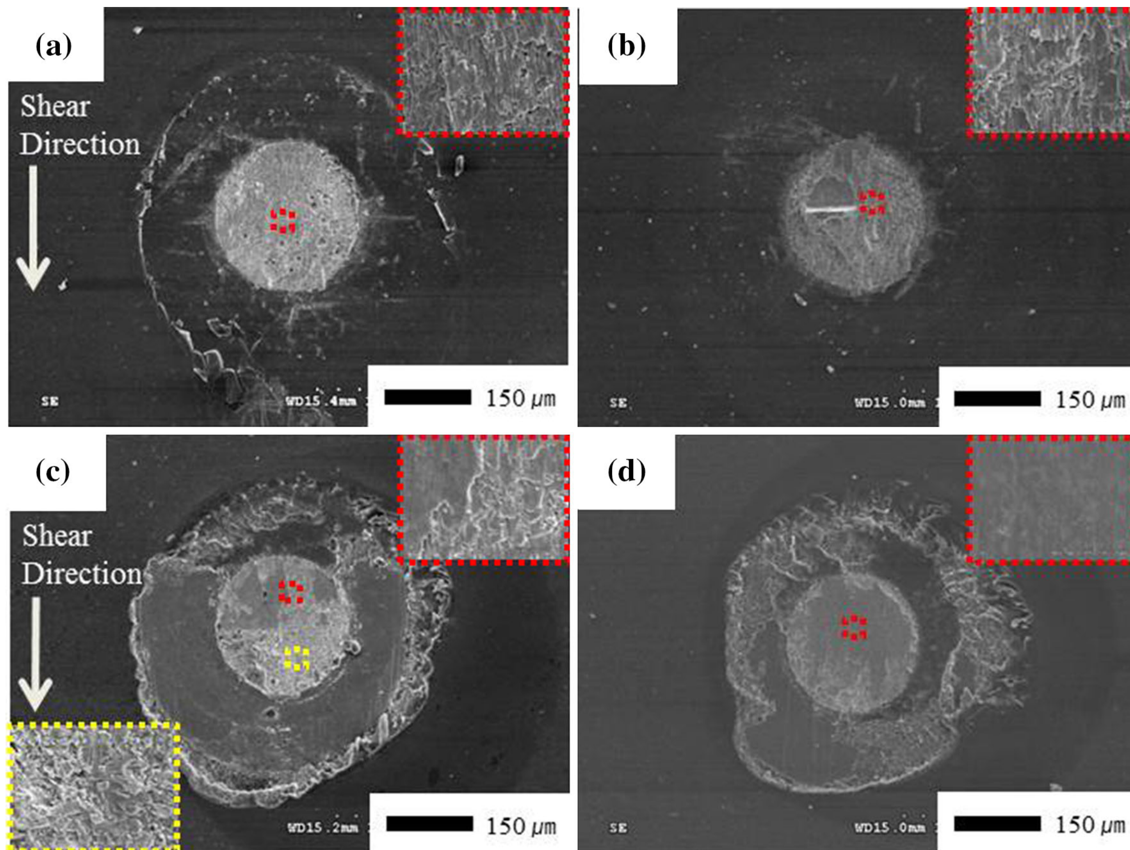

Fig. 4. SEM Micrographs of top view of fractured surfaces after the shear test; (a) SB-ENIG, (b) SB-ENEPIG, (c) SBE-ENIG, (d) SBE-ENEPIG.

our previous study (SBE[25]), the SBE-ENIG and SBE-ENEPIG samples even showed decreased values, indicating the negative effect of ENIG and ENEPIG surface finishes in cases of epoxy-enhanced solder joints. ENIG and ENEPIG surface finishes have been the successfully applied methods for the bonding strength enhancement of solder joints for Sn-based solders in the electronic industries.[4,6,10,27,28]

To understand these discrepancies of surface finishes due to epoxy addition, the fracture surfaces of both the board side and the solder side of the samples after the drop test were investigated. Figures 6 and 7 show the morphologies and chemical compositions of SBE-ENIG and SBE-ENEPIG, respectively. Disk-shaped and dark spots were observed from all surface finished samples, showing the well-defined edges of spots and much darker areas inside the spots, indicating that the epoxy remnant was possibly trapped inside the solders and formed a disk-shaped void with an epoxy-condensed puddle after reflow. These dark spots were observed in all

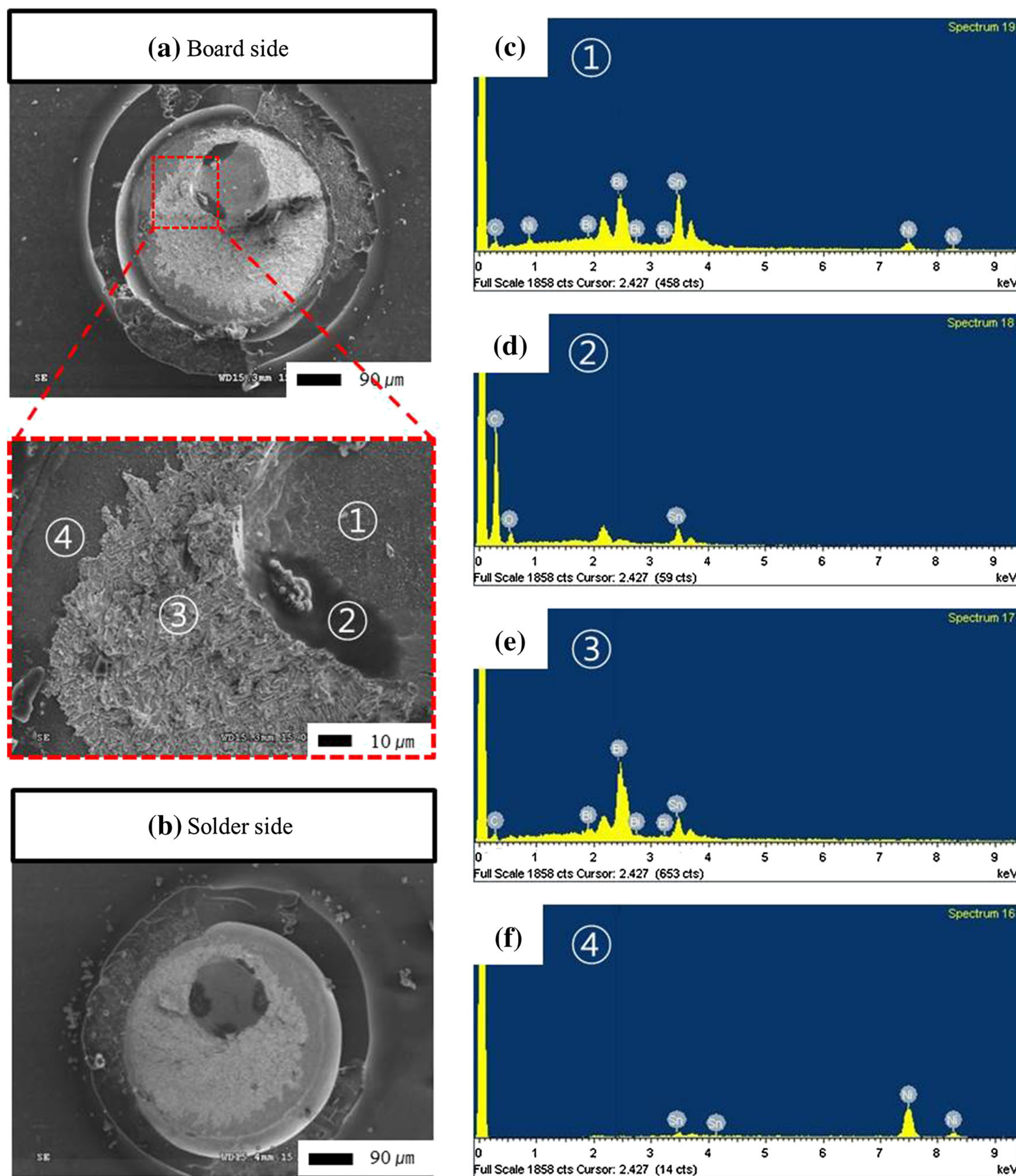

Fig. 6. SEM micrographs of fracture surfaces after drop tests with EDS spectra collected from the corresponding positions (sample: SBE-ENIG); (a) board side, (b) solder side, (c) IMC layer, (d) carbon trace, (e) Sn-Bi solder, (f) Ni-P layer.

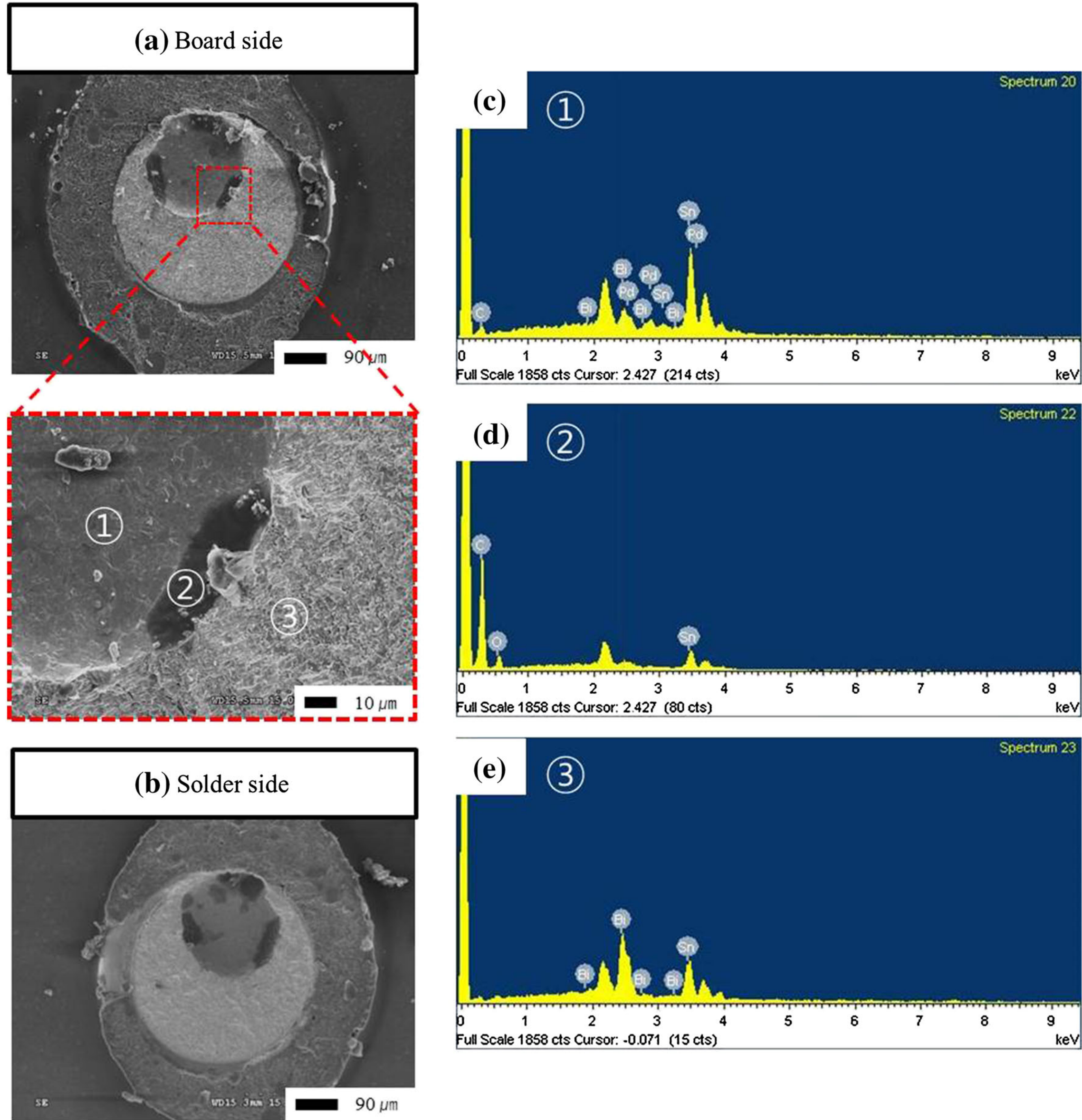

Fig. 7. SEM micrographs of fracture surfaces after drop tests with EDS spectra collected from the corresponding positions (sample: SBE-ENEPIG); (a) board side, (b) solder side, (c) IMC layer, (d) carbon trace, (e) Sn-Bi solder.

ENIG/ENEPIG surface-finished samples. EDS measurements also showed carbon traces on these spots and relatively strong peaks on the darker area inside the spot (② in Figs. 6 and 7). It is thereby expected that, if the entire epoxy is not consumed from the solder matrix to form the epoxy wall around the solder during reflow, the remained epoxy inside the solder agglomerates and forms a puddle of an epoxy-void mixture, eventually shown as a dark spot after fracture of the solder. Ni and Ni-Pd usually form the intermetallic compound (IMC) at the interfaces of Sn-based solder joints during reflow, and these IMC layers can possibly act as a barrier for epoxy to smear out completely from the solder matrix, and thereby induce the trapping of a puddle of epoxy-void mixture before solidification of the epoxy solders. It was expected that curing of epoxy in the solder (smearing-out from the solder) was thought to be relatively slow compared to the formation of Au- and Pd-based IMC's and, therefore, these IMCs trapped the epoxy and, as a result, dark spots with/without voids formed inside the solder/ENIG and ENEPIG joints. To confirm this explanation, further study is needed with a variation in reflow time. Additionally, in the SBE-ENIG sample, some fracture surface areas on the bonding pad showed no or little solder trace and a strong Ni peak (④ in Fig. 6), indicating that the bonding was not strong between the epoxy solder and the ENIG surface-finished bonding pad. Considering these morphological aspects (no clear effects in the shear test and lower numbers in the drop test of SBE-

ENIG/SBE-ENEPIG samples), careful application of surface finishes is needed due to the undesirable interfacial reactions between the epoxy and the metal bonding pad (Cu, Ni, and Pd). In other words, besides the polymer–polymer (epoxy versus SR) bonding enhancement, the polymer–metal bonding (epoxy versus Cu- or Ni/Pd-layered bonding pads with surface finishes) should be designed depending on the reflow conditions. In order to minimize the undesirable polymer–metal reaction between the epoxy and the metallic bonding pad, a prolonged reflow time, a slightly higher reflow temperature or temperature/reflow time combination, can be selected for the complete smearing-out of the epoxy from the solder matrix.

Figure 8 shows SEM micrographs of solder–bonding pad interfaces of the SB/SBE samples with ENIG and ENEPIG surface finishes, respectively. As expected, the formation of IMCs at the interfaces was observed in all samples, regardless of whether or not they contained epoxy: Ni_3Sn_4 in ENIG- and $(Ni,Pd)_3Sn_4$ in ENEPIG-finished samples, respectively. The average values of the measured thicknesses of the IMCs are also shown below the respective SEM micrographs. The SBE samples showed relatively thinner thicknesses of IMCs compared to those of the SB samples, indicating that the remaining epoxy inside the solder may restrain the growth of IMCs. The restraining role of epoxy on the growth of IMCs at the interfaces was also observed in the elementary mapping as shown in Fig. 9. The IMCs were primarily composed of Sn and Ni in the SB/SBE-ENIG, and Sn and (Ni, Pd) in the SB/SBE-ENEPIG samples, respectively. As expected, no trace of Bi was found in the formation of IMCs in any sample.[29,30] Even though it is difficult to measure the C contents accurately with EDS or EPMA analyses due to the inherited limited detection capability for light elements, a relative mapping contrast was observed between the solder matrix and the bonding pad, indicating the remaining epoxy in the solder matrix after reflow,

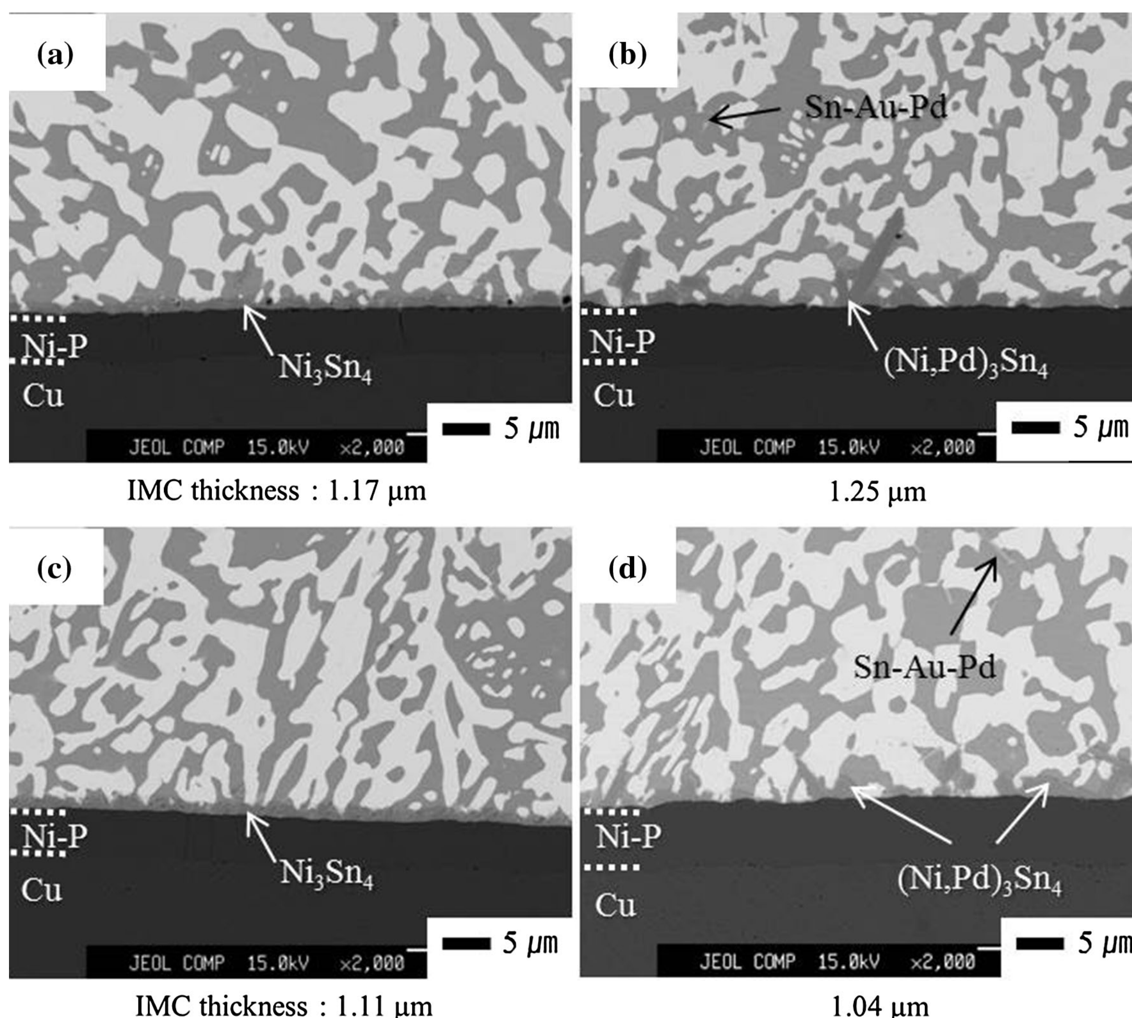

Fig. 8. SEM micrographs of solder–bonding pad interfaces with ENIG and ENEPIG surface finishes, showing formation of IMCs at the interfaces; (a) SB-ENIG, (b) SB-ENEPIG, (c) SBE-ENIG, (d) SBE-ENEPIG.

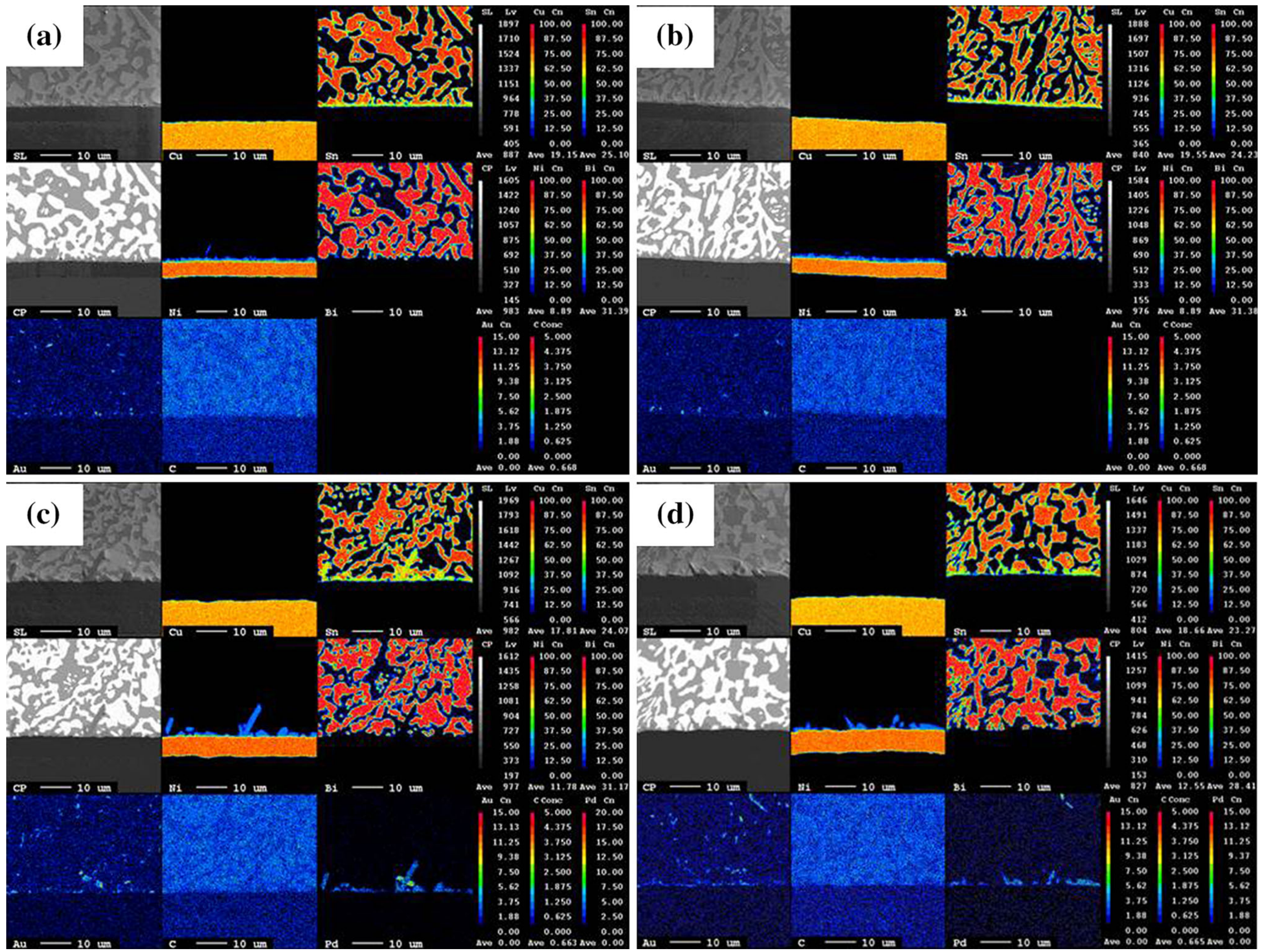

Fig. 9. Elementary mapping of solder–bonding pad interfaces; (a) SB-ENIG, (b) SBE-ENIG, (c) SB-ENEPIG, (d) SBE-ENEPIG.

since the major composition of epoxy is C, O, and H.[31] It was also shown that the addition of epoxy did not alter the morphologies of the IMCs at the interfaces (roughened-layer type in SB/SBE-ENIG and the needle-like type in SB/SBE-ENEPIG samples), and again rather smaller and thinner IMCs were observed in the samples with an epoxy addition. The long-term effects of epoxy on the IMC growth and thereby the overall effects on the mechanical properties of SBE solders will be discussed in a following study.

CONCLUSION

The effects of two surface finishes, ENIG and ENEPIG, on the mechanical properties and microstructures of epoxy-enhanced Sn-58Bi solder joints were investigated using a low-speed shear test and the board level drop test, followed by microchemical analyses. It was shown that, in the low speed shear test, the addition of epoxy in the Sn-58Bi solder exhibited an enhanced bonding strength of the solder joints regardless of the type of applied surface finish. However, in the samples with epoxy, the results of the drop test showed the negative effects of ENIG and ENEPIG surface finishes on the bonding strength. This discrepancy in the results of the two mechanical tests originated from the difference in the relative ratio of bonding areas between the epoxy–SR bonding and solder–bonding pad bonding. In the current reflow condition (190°C for 5 min), the epoxy was not completely dissolved from the solder matrix and caused relatively poor bonding of the solder with the Ni- and Pd-finished bonding pad. The remaining epoxy in the solder matrix also restrained the formation of IMCs in the cases of ENIG and ENEPIG surface finishes. As a result, ENIG and ENEPIG surface finishes on the solder joints with epoxy should be applied with carefully designed reflow conditions so as to dissolve the epoxy completely from the solder–bonding pad interfaces and not overgrow the IMCs due to the prolonged reflow time.

ACKNOWLEDGEMENTS

This work was supported by the Human Resources Program in Energy Technology of the Korea Institute of Energy Technology Evaluation and Planning (KETEP) granted financial resource from the Ministry of Trade, Industry & Energy, Republic of Korea (20154030200870).

REFERENCES

1. Directive 2002/95/EC, The Restriction of the Use of Certain Hazardous Substances in Electrical and Electronic Equipment, The European Parliament and of the Council of the European Union, 27 January 2003.
2. Directive 2002/96/EC, Waste Electrical and Electronic Equipment (WEEE), The European Parliament and of the Council of the European Union, 27 January 2003.
3. B. Sandy, E. Briggs, and R. Lasky, Indium Corporation Tech Paper No. 1 (2011). http://www.indium.com/techlibrary/whitepapers/advantages-of-bismuthbased-alloys-for-low-temperature-pbfree-soldering-and-rework.
4. J.H. Kim, Y.C. Lee, S.M. Lee, and S.B. Jung, *Microelectron. Eng.* 120, 77 (2014).
5. X. Hu, X. Yu, Y. Li, Q. Huang, Y. Liu, and Z. Min, *J. Mater. Sci. Mater. Electron.* 25, 57 (2014).
6. J.W. Yoon and S.B. Jung, *J. Alloys Compd.* 359, 202 (2003).
7. H. Chen, J. Han, J. Li, and M. Li, *Microelectron. Reliab.* 52, 1112 (2012).
8. H.X. Xie and N. Chawla, *Microelectron. Reliab.* **53**, 733 (2013).
9. S.S. Ha, J.Y. Sung, J.W. Yoon, and S.B. Jung, *Microelectron. Eng.* 88, 709 (2011).
10. J.W. Yoon, B.I. Noh, and S.B. Jung, *J. Electron. Mater.* 40, 1950 (2011).
11. H.W. Miao and J.G. Duh, *Mater. Chem. Phys.* 71, 255 (2001).
12. X.F. Li, F.Q. Zu, H.F. Ding, J. Yu, L.J. Liu, and Y. Xi, *Phys. Lett. A* 354, 325 (2006).
13. Q.K. Zhang and Z.F. Zhang, *Mater. Sci. Eng. A* 528, 2686 (2011).
14. B.L. Young, J.G. Dug, and G.Y. Jang, *J. Electron. Mater.* 32, 1463 (2003).
15. M.S. Suh, C.J. Park, and H.S. Kwon, *Surf. Coat. Technol.* 200, 3527 (2006).
16. M.S. Suh, C.J. Park, and H.S. Kwon, *Mater. Chem. Phys.* 110, 95 (2008).
17. T. Kotake, H. Murai, S. Takanezawa, M. Miyatake, M. Takekoshi, and M. Ose, *CPMT Symposium Japan (ICSJ)* (Kyoto, Japan, 2013), pp. 1–4.
18. J.N. Choi, M.K. Ko, S.M. Lee, and S.B. Jung, *J. Microelectron. Packag. Soc.* 20, 1 (2013).
19. K. Suganuma, T. Sakai, K.S. Kim, Y. Takagi, J. Sugimoto, and M. Ueshima, *IEEE Trans. Electron. Packag. Man.* 25, 257 (2002).
20. W. Dong, Y. Shi, Z. Xia, Y. Lei, and F. Guo, *J. Electron. Mater.* 37(7), 982 (2008).
21. J.S. Hwang, Environment-Friendly Electronics: Lead-Free Technology, Electrochemical Publications, LTD, Isle of Man, Great Britain, 31 Chapters, 2001 (ISBN-0-90-115040-1).
22. C. Wu, J. Shen, and C. Peng, *J. Mater. Sci. Mater. Electron.* 23, 14 (2012).
23. C. Fuchs, T. Schreck, and M. Kaloudis, *J. Mater. Sci.* 47, 4036 (2012).
24. S.T. Oh and J.H. Lee, *Electron. Mater. Lett.* 10(2), 473 (2014).
25. W.R. Myung, Y. Kim, and S.B. Jung, *J. Alloys Compd.* 615, S411 (2014).
26. R. Darveaux and C. Reichman, *Electronics Packaging Technology Conference* (Singapore, 2006), pp. 283–289.
27. S.P. Peng, W.H. Wu, C.E. Ho, and Y.M. Huang, *J. Alloys Compd.* 493, 431 (2010).
28. P. Snugovsky, P. Arrowsmith, and M. Romansky, *J. Electron. Mater.* 30(9), 1262 (2001).
29. D.J. Chakrabarti and D.E. Laughlin, *Bull. Alloy Phase Diagr.* 5, 148 (1984).
30. Z. Mei and J.W. Morris Jr., *J. Electron. Mater.* 21, 599 (1992).
31. Y. Tanaka, *Epoxy Resins Chemistry and Technology, Chapter 2: Synthesis and Characterization of Epoxides* (Marcel Dekker, New York, 1988), pp. 54–63.